Sādhanā Vol. 40, Part 2, April 2015, pp. 467–485. © Indian Academy of Sciences

Laminar flow heat transfer studies in a twisted square duct for constant wall heat flux boundary condition

RAMBIR BHADOURIYA, AMIT AGRAWAL and S V PRABHU*

Department of Mechanical Engineering, Indian Institute of Technology,
Bombay 400 076, India
e-mail: svprabhu@iitb.ac.in

MS received 18 April 2014; revised 25 August 2014; accepted 20 November 2014

Abstract. The problem of fluid flow and heat transfer was studied for flow inside twisted duct of square cross-section. Three-dimensional numerical solutions were obtained for steady fully developed laminar flow and for uniform wall heat flux boundary conditions using commercially available software. Reynolds number range considered was 100–3000. Twist ratio used are 2.5, 5, 10 and 20. Fluids considered are in Prandtl number range of 0.7–20. Product of friction factor and Reynolds number is found to be a function of Reynolds number and maximum values are observed for a twist ratio of 2.5 and Reynolds number of 3000. Maximum Nusselt number is observed for the same values along with Prandtl number of 20. Correlations for friction factor and Nusselt number are developed involving swirl parameter. Local distribution of friction factor ratio and Nusselt number across a cross-section is presented. Based on constant pumping power criteria, enhancement factor is defined to compare twisted ducts with straight ducts. Selection of twisted square duct is presented in terms of enhancement factor. It is found that twisted duct performs well in the laminar region for range of parameters studied. Heat transfer enhancement for Reynolds number of 3000 and Prandtl number of 0.7 for twist ratio of 2.5, 5, 10, and 20 is 20%, 17.8%, 16.1% and 13.7%, respectively. The results are significant because it will contribute to development of energy efficient compact size heat exchangers.

Keywords. Heat transfer; laminar flow; twist ratio; periodic flow; twisted duct; enhancement.

1. Introduction

In process industry, there is constant emphasis to increase the thermal performance of heat exchangers thereby contributing to material, energy and floor space saving. Performance of conventional heat exchangers can be improved by number of enhancement techniques. Heat transfer enhancement techniques can be classified either as passive, which require no direct application

---

*For correspondence

of external power, or as active, which require external power. Some application requires combination of both active and passive techniques. Selection of particular technique depends on the thermal hydraulic goals such as reducing size of heat exchangers or reducing temperature approach. Twisted duct works on the principle of passive enhancement technique in which heat transfer enhancement is created by generating swirl in flow. Heat transfer augmentation obtained is similar to twisted tape in straight ducts. Twisted duct used in heat exchanger not only enhances heat transfer inside the ducts, but also for shell side fluid in duct to duct space of heat exchanger bundle.

Todd (1977) studied steady laminar flow in twisted pipes with elliptical cross section.

He considered rigid pipe of straight centreline and fixed cross-sectional geometry. Twist effect is taken into consideration by varying orientation of cross section along the length of pipe modelling the problem with larger twist ratio. The author defined the large twist ratio as ratio when change in twist angle (θ) of cross-section of duct with respect to the direction of flow (z) is very small ($d\theta/dz \ll 1$). He derived a fourth order partial differential equation for the stream function and showed that it is identical to the equation for the small transverse displacement of a clamped elastic plate under a constant loading. Although, this analysis is applicable for a pipe of any cross-section with proper boundary conditions, its validity is limited only to a large twist ratio elliptic pipe. Masliyah & Nandakumar (1981a, b) numerically studied the friction factor and heat transfer data for the fully developed steady laminar flow through twisted square ducts with rotation coordinates system. The temperature at each wall was considered constant. However, axial conduction in fluid was neglected along the flow direction. Enhancement was only observed for twist ratio 2.5 and for Reynolds number range of 1–1000. Similar expected enhancement was not observed for higher twist ratios (5–20) studied by author. Later Xu & Fan (1986) suggested correction in the viscous dissipation term used by Masilyah & Nandakumar (1981a, b).

Chang *et al* (1988) used numerical method to study laminar flow in a twisted elliptic tube for large twist ratios ($H = 21, 53, 106$). Effect of twist ratio and aspect ratio of ellipse on axial and circumferential velocity profile is analysed. Bishara (2010) numerically investigated laminar fully developed flow in elliptical tubes for *Re* range of 10–1000 and *Pr* of 3. Elliptical tubes with aspect ratio of 0.3, 0.5 and 0.7 and twist ratio of 6, 9 and 12 were considered. Twisted elliptical tube showed considerable heat transfer enhancement compared to straight tube. Yang *et al* (2011) experimentally evaluated performance of five twisted elliptical tubes. Aspect ratio (major diameter/minor diameter) of elliptical tubes used was in the range 1.49–2.15 and twist ratio range covered was 17.4–32.8. Water was used as the working fluid for *Re* range of 600–55000 covering laminar, transition and turbulent regime. They concluded that for twisted duct flow remains laminar for $Re \leq 2300$. In twisted tube heat transfer enhancement is higher for laminar regime compared to transition and turbulent flow regime.

Based on the literature studied by research it can be concluded that limited studies are available for flow in twisted tubes. Results available are individually separate and do not cover the wide range of *Re* and *Pr*, although twisted elliptical tubes received more attention compared to twisted square ducts. Results available for twisted elliptical tubes are limited to *Re* range of 10–1000 and *Pr* range of 3–5. Twist ratios studied are in the range of 6–106. Even for elliptical tubes numerical solution for entire laminar flow regime is not available. *Pr* range studied is narrow and does not cover many fluids practically used in heat exchangers. Twist ratios studied for elliptical tubes are of larger twist ratios which are not much effective for enhancing heat transfer. Mechanism of heat transfer enhancement is not addressed in the literature. Square twisted duct does not receive much attention in the literature. Analysis of twisted square duct with constant wall heat flux boundary condition is work of its first kind. Hence there is a need for an equation to predict friction factor and heat transfer solution for a wide range of Reynold number and Prandtl number.

In the present paper three dimensional fully developed laminar flow study is done to investigatethe pressure drop and heat transfer in twisted square duct. *Re* range considered was 100–3000 and *Pr* range was 0.7–20. Twist ratios studied were 2.5–20. Numerical analysis is

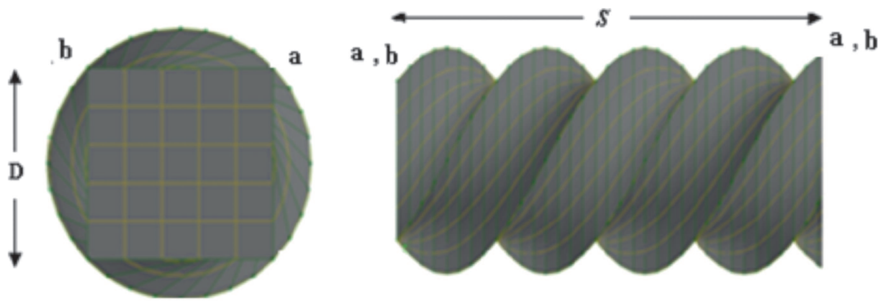

(a) **Terminologies (*H* = 2.5)**

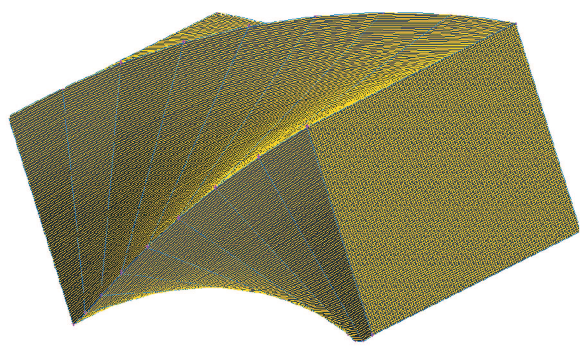

(b) **Computational mesh (*H* = 2.5)**

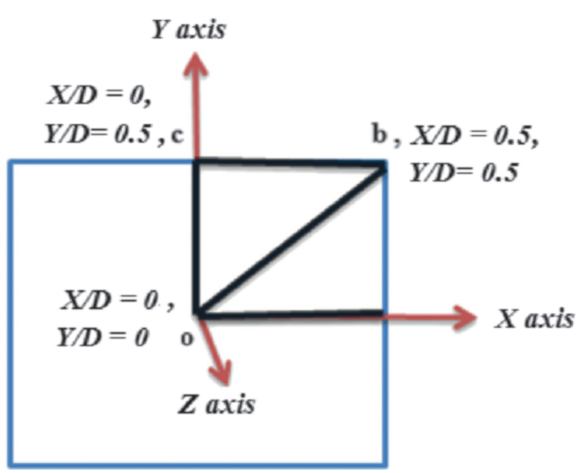

(c) **Cross section of Square duct**

Figure 1. Twisted square duct.

done with help of FLUENT, a widely accepted CFD tool. Local distribution of friction factor and Nusselt number in duct cross section are provided to explain mechanism of heat transfer enhancement. Objective is to generate correlations to predict friction factor and Nusselt number for entire range of parameters studied.

2. Definitions

Common terminologies used with twisted duct have been shown in figure 1a are as follows:

- Pitch (S): It is the distance between two consecutive points along the length of tube where the orientation of tube cross section exactly coincides with each other. Cross section rotates by 360° along one pitch distance.
- Twist ratio (H): It is the geometrical parameter used to describe flow through twisted ducts. It is defined as the ratio of the pitch (S) to hydraulic diameter (d) of the duct. Higher H indicates mild twist and lower H indicates severe twist.

3. Numerical methodology

FLUENT software (version 6.2.16) has the ability to provide solution of fluid flow and heat transfer by using periodic flow concept. Periodic flow concept in FLUENT is widely utilized for numerical calculations when the geometry of model is made of repeated module of some length L, with a constant pressure drop across each repeating module along the flow direction. In such case fully developed solutions can be obtained in FLUENT by modelling a single module. In the present cases of twisted square duct, length (S/4) of twisted duct was considered and periodic flow concept was utilized to obtain the solution. This permits the use of a scaled model and reduces the computational time. However numerical solutions obtained are of fully developed flow. As present work is the first of its kind, hence for analysis purpose flow is assumed to be laminar for Re of 3000 similar to flow in straight duct. Prandtl numbers considered are 0.7, 5, 10, 15 and 20. Twist ratio considered is 2.5, 5, 10 and 20. Three dimensional models are used in the analysis with hexahedron mesh elements. Peripherally and axially uniform wall heat-flux boundary conditions are used. Body forces due to gravity are neglected. Solutions are obtained for steady state, incompressible, hydrodynamically and thermally developed flow. Common calculation methodology adopted in the present study is one case ($H = 2.5$, $Re = 3000$ and $Pr = 0.7$) of solution is presented. Twisted square duct ($H = 2.5$) of periodic Length ($S/4$) is meshed with hexahedron elements. Three meshes with elements 40000, 60000 and 80000 are generated. Figure 1b shows meshed model for twist ratio 2.5 with 80000 elements. Fluid flow and heat transfer solution is obtained as per the parameters listed in table 1. Wall temperature (T_w), bulk temperature (T_b), heat flux (q'') and shear stress (τ_w) data are obtained at different locations along the length of the duct. Friction factor can be obtained from wall shear stress as

$$\mathrm{f} = \frac{\tau_w}{\left(\frac{\rho \mathrm{V_m}^2}{2}\right)}. \tag{1}$$

Table 1. Parameters used in FLUENT.

Models	Solver	Segregated
	Formulation	Implicit
	Space	3D
	Time	Steady
	Viscous model	Laminar
Boundary conditions	Inlet	Periodic
	Outlet	Periodic
	Wall	Constant temperature
	Periodic type	Translational
	Periodicity condition	Mass flow specified
Discretization	Pressure	Second order
	Momentum	Second order upwind
	Energy	Second order upwind
	Pressure–velocity coupling	Simple
Convergence	Continuity	10^{-7}
	Velocity	10^{-6}
	Energy	10^{-7}

Table 2. Grid Independence results for $H = 2.5$, $Re = 3000$ and $Pr = 0.7$.

Models	Element	$\bar{f}$Re	$(\overline{Nu_q})_{tw}$
Mesh 1	40000	61.22	33.27
Mesh 2	60000	63.67	34.32
Mesh 3	80000	63.61	34.62

Heat transfer coefficient (h) and Nusselt number (Nu) were calculated at each location along the length of tube and around wall

$$\mathrm{h} = \frac{\mathrm{q}''}{(T_{\mathrm{w}} - \mathrm{T_b})}, \tag{2}$$

$$\mathrm{Nu} = \frac{\mathrm{h.d}}{\mathrm{k}}. \tag{3}$$

Average fluid flow and Nusselt number results are provided in table 2. Difference in results between mesh 2 and mesh 3 is less than 1%. Hence, the results of mesh 3 with 80000 elements are considered as the results for case of $H = 2.5$, $Re = 3000$ and $Pr = 0.7$. In similar way, results are obtained for twist ratio 5, 10, and 20 using mesh with hexahedron element 1,20,000, 1,40,000, and 1,80,000, respectively. Machine used for computation is Intel core 2 Duo processor with speed of 2.6 GHz.

4. Average friction factor

Numerical friction factor solution for different twist ratios are presented in figure 2. It is seen that $\overline{(f\ Re)}_{tw}$ values for twisted duct are functions of both Re and H, unlike a straight tube where

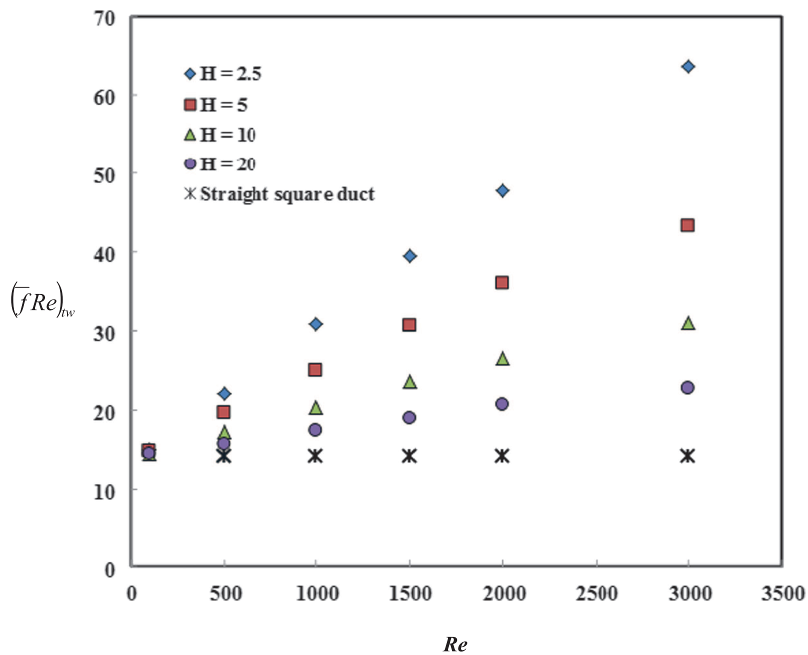

Figure 2. Numerical friction factors for the laminar flow regime.

$\overline{(f\ Re)}_{st}$ is independent of Re and remains constant in the laminar flow regime. The maximum value of $\overline{(f\ Re)}_{tw}$ is 63.6 obtained for a twist ratio of 2.5 at $Re = 3000$. This dependence of $\overline{(f\ Re)}_{tw}$ values is attributed to the presence of swirl flow in the twisted duct. Hence effort is made to correlate friction factor in terms of swirl factor. An effort is made to collapse all the data onto a single curve, by introducing a swirl parameter. Manglik & Bergles (1993) had introduced swirl parameter for twisted tape. Twisted duct imparts swirl to fluid due to duct geometry similar to tape inserts in duct. Hence the swirl parameter (*Sw*) for twisted duct is introduced here is a modified form of swirl parameter for twisted tape suggested by Manglik & Bergles (1993) and defined by Eq. (4).

$$\mathrm{Sw} = \frac{\mathrm{Re}}{\sqrt{\mathrm{H}}} \mathrm{A}_r. \tag{4}$$

The swirl parameter is a function of Reynolds number and area ratio and inversely proportional to the square root of twist ratio. A_r in Eq. (4) is defined as

$$\mathrm{A_r} = \frac{\mathrm{A_{st}}}{\mathrm{A_{tw}}}. \tag{5}$$

Physically, it is heat transfer area ratio of twisted tube to its untwisted counterpart having the same flow cross section area and the same flow length. The straight square duct heat transfer area, A_{st} is given by Eq. (6)

$$\mathrm{A_{st}} = 4\,\mathrm{Sd_h}, \tag{6}$$

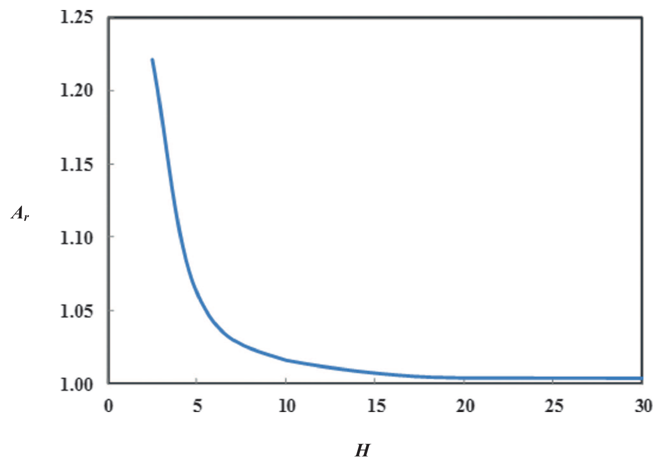

Figure 3. Effect of twist ratio on heat transfer area.

while the heat transfer area for twisted square duct, A_{tw} can be obtained from Eq. (7)

$$\mathrm{A_{tw}} = 4\pi\, \mathrm{d_h^2}\left[0.5\left(1+\frac{\mathrm{H}^2}{\pi^2}\right)+\frac{\mathrm{H}^2}{2\pi^2}\ln\left\{\frac{\pi}{\mathrm{H}}+\left(1+\frac{\pi^2}{\mathrm{H}^2}\right)^{\frac{1}{2}}\right\}\right]. \tag{7}$$

A_r obtained from Eq. (5) is presented through figure 3. It is observed that the area ratio decreases with the increase in the twist ratio. Hence, not much advantage is obtained by employing twisted duct having H greater than 20 for heat transfer enhancement. Numerical data for $\overline{(f\ Re)}_{tw}$ can be correlated in terms of swirl parameter *Sw* for a twisted duct as shown in figure 4. *Sw* is a modified form of Correlation (based on 25 data points) obtained is given by Eq. (8) and predict values within 5% of the actual numerical values.

$$\overline{(\mathrm{f.Re})}_{\mathrm{tw}} = 0.0217\mathrm{Sw} + 14.2, \tag{8}$$

$$(100 \le Re \le 3000) \text{ and } (2.5 \le H \le 20).$$

Eq. (8) shows a linear dependence of *f.Re* on swirl parameter.

5. Average heat transfer

Heat transfer solutions are obtained for uniform wall heat flux boundary condition. *Pr* values considered are 0.7, 5, 10, 15 and 20. Figures 5 and 6 show $\overline{(Nu_q)}_{tw}$ values for *Pr* of 0.7 and 20, respectively. Similar to $\overline{(f\mathrm{Re})}_{tw}$ values, $\overline{(Nu_q)}_{tw}$ values also show dependence on *Re* and H unlike straight square duct for which Nusselt number values remain constant in the laminar flow regime. Similar to $\overline{(f\ Re)}_{tw}$ values, $\overline{(Nu_q)}_{tw}$ values also show dependence on *Re* and H unlike straight square duct for which Nusselt number values remain constant in the laminar flow regime. For a given *Re* and *Pr*, $\overline{(Nu_q)}_{tw}$ increases with a decrease in H; this is expected owing to an increase in the magnitude of secondary flow. Also for a given H and *Pr*, $\overline{(Nu_q)}_{tw}$ increases with *Re*. Figure 5 shows that for *Pr* value of 0.7, $\overline{(Nu_q)}_{tw}$ has a linear dependence on *Re* for all twist ratios. It is however observed from figure 6 that for *Pr* value of 20, $\overline{(Nu_q)}_{tw}$ exhibits a

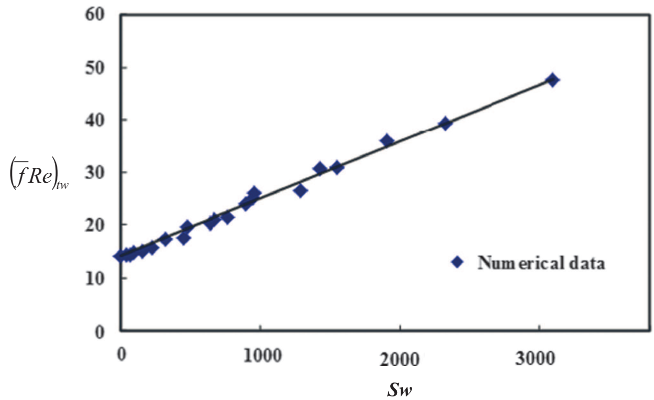

Figure 4. Variations of average friction factor with swirl parameter (Laminar flow).

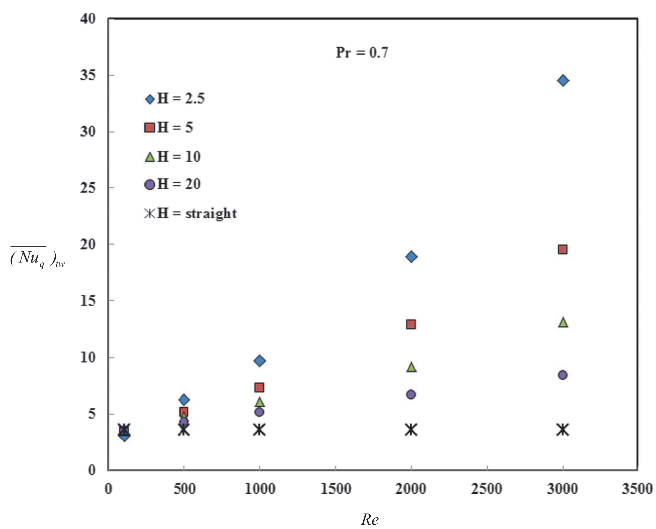

Figure 5. Heat transfer solution for $Pr = 0.7$.

linear dependence on *Re* only for large twist ratios. The maximum value of $\overline{(Nu_q)}_{tw}$ obtained is 741.7 with $H = 2.5$, $Pr = 20$ and $Re = 3000$.

Similar to $\overline{(f\ Re)}_{tw}$ correlation, swirl parameter *Sw* is employed here to collapse all data points onto a single curve. Numerical data (based on 125 data points) of $\overline{(Nu_q)}_{tw}$ at different *Pr* was correlated Eq. (9) predicts Nusselt number values with average deviation of 5.2% accuracy of numerical data.

$$\overline{(\mathrm{Nu_q})}_{tw} = 0.0004\ Sw^{1.5}\ \mathrm{Pr} + 3.6. \tag{9}$$

6. Results and discussion

In the previous section, $\overline{(f\ \mathrm{Re})}_{tw}$ and $\overline{(Nu_q)}_{tw}$ values calculated for twisted square duct were dependent on *Re*, *Pr* and *H* values, which is contrary to straight square duct for which $\overline{(f\ \mathrm{Re})}_{st}$

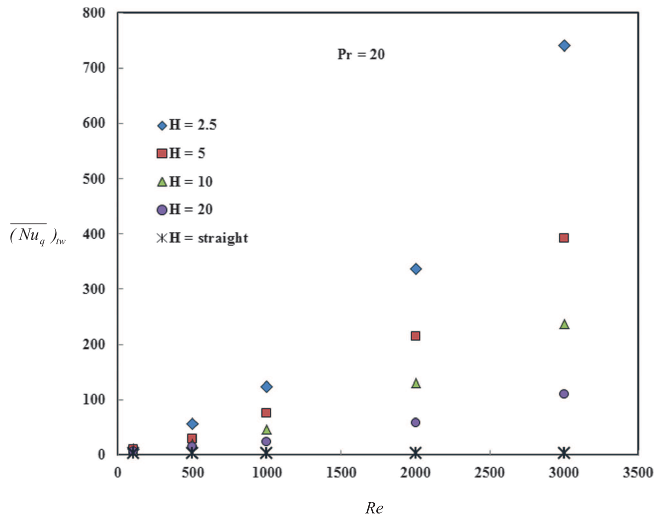

Figure 6. Heat transfer solution for $Pr = 20$.

and $\overline{(Nu_q)}_{st}$ remain constant in the laminar flow regime. In this section, local variation of $(f\,Re)_{tw}$ and $(Nu_q)_{tw}$ is studied. Figure 1c shows cross-section of square tube. Z axis is along the flow direction while X and Y axes are in the cross-sectional plane. Line *cb* represents half edge of the square side. Line *oc* and line *ob* are along half-side and half-diagonal of cross-section with o as center of cross-section.

6.1 *Local friction factor variation*

Figure 7 shows local $(f\mathrm{Re})_{tw}$ variation along half edge *cb* for twist ratio 10. In straight tube, the maximum $(f\mathrm{Re})_{tw}$ occurs at the centre of side of duct and zero at corner. However, for twisted duct, location of the maxima is a function of Reynolds number; it shifts away from the centre of

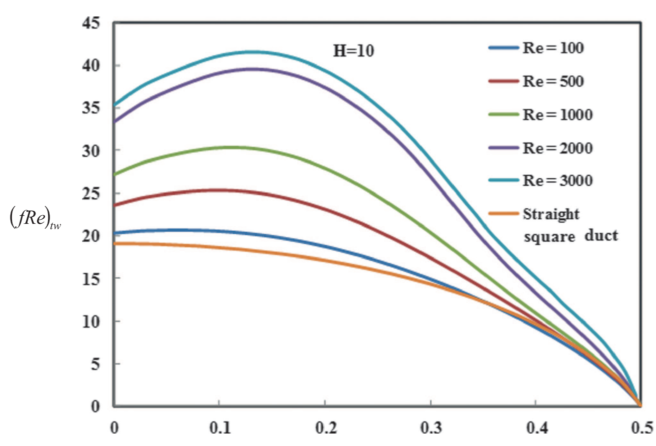

Figure 7. Variation of local *f.Re* along the wall (cb) for $H = 10$.

the side with an increase in Re. This is attributed to the presence of secondary flow in the twisted duct. Figure 8 shows contours of dimensionless x velocity (V_x/V_{mi}) for different twisted ratios at $Re = 1000$. It shows the presence of strong secondary flow near the wall region. Also, it is seen that the magnitude of secondary flow is higher for small twist ratio. To analyse it further V_x and V_z components of velocity are plotted for different twist ratios. Figures 9 and 10 show V_x and V_z components of velocity respectively along line *ob*. The velocities are non-dimensionalized with respect to the mean inlet velocity (V_{mi}). It is seen from figure 9 that the secondary flow reduces with an increase in twist ratio. From figure 10 it is observed that maximum V_z occurs

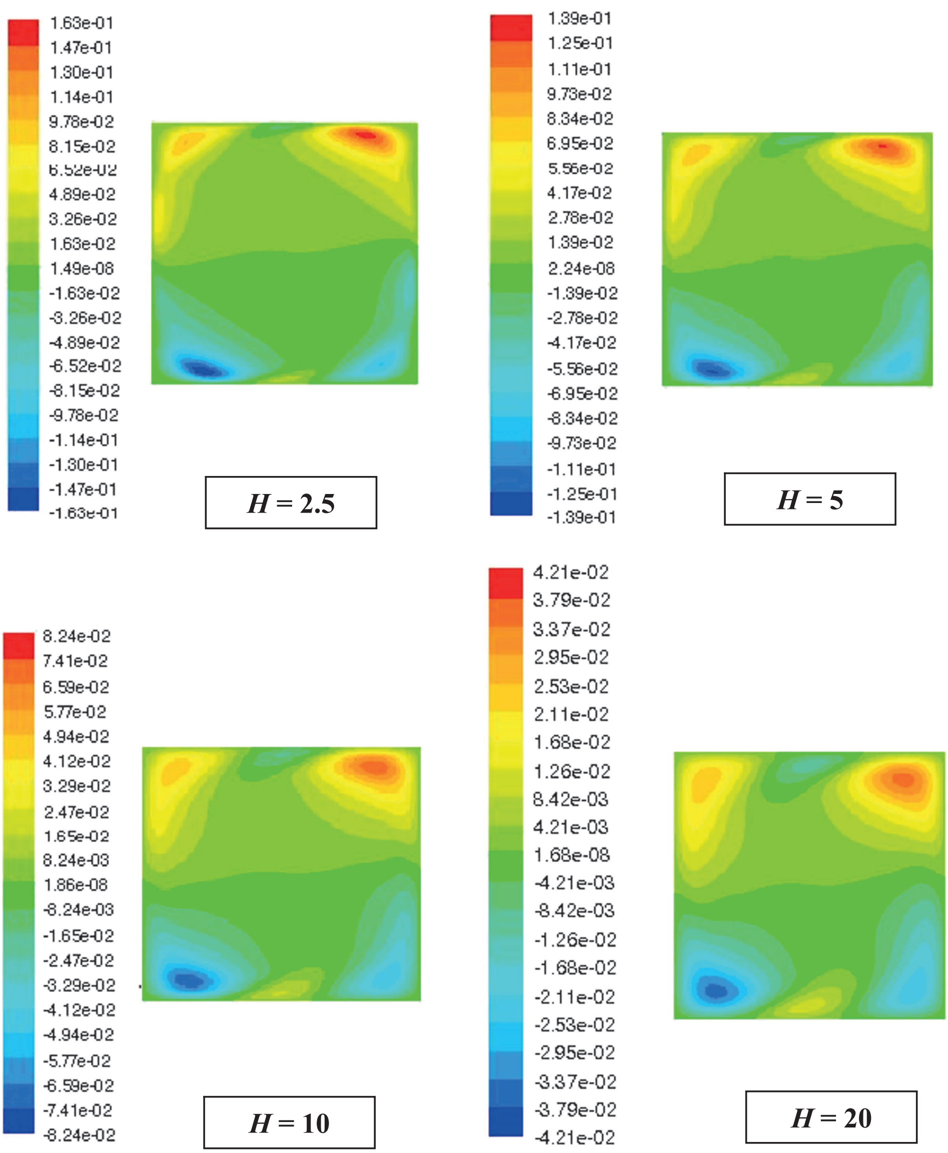

Figure 8. Contours of non-dimensional x velocity (V_x/V_{mi}) for a different twist ratio at $Re = 100$.

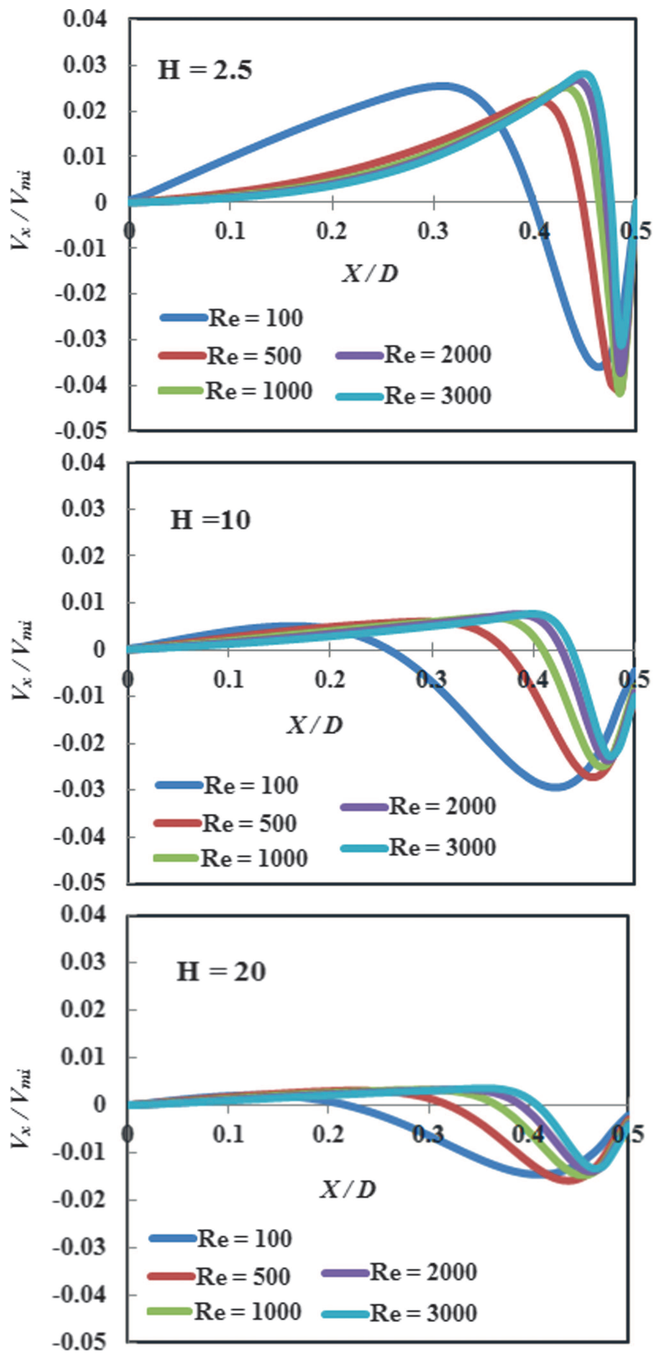

Figure 9. Effect of twist ratio on secondary flow (line ob).

at the center of duct and it is 2.1 times that mean inlet velocity or mean velocity at given cross section for $H = 2.5$ and $Re = 3000$. It can be concluded that V_x (same as V_y) component of velocity is mainly responsible for creating swirl in flow and it is more effective at smaller twist

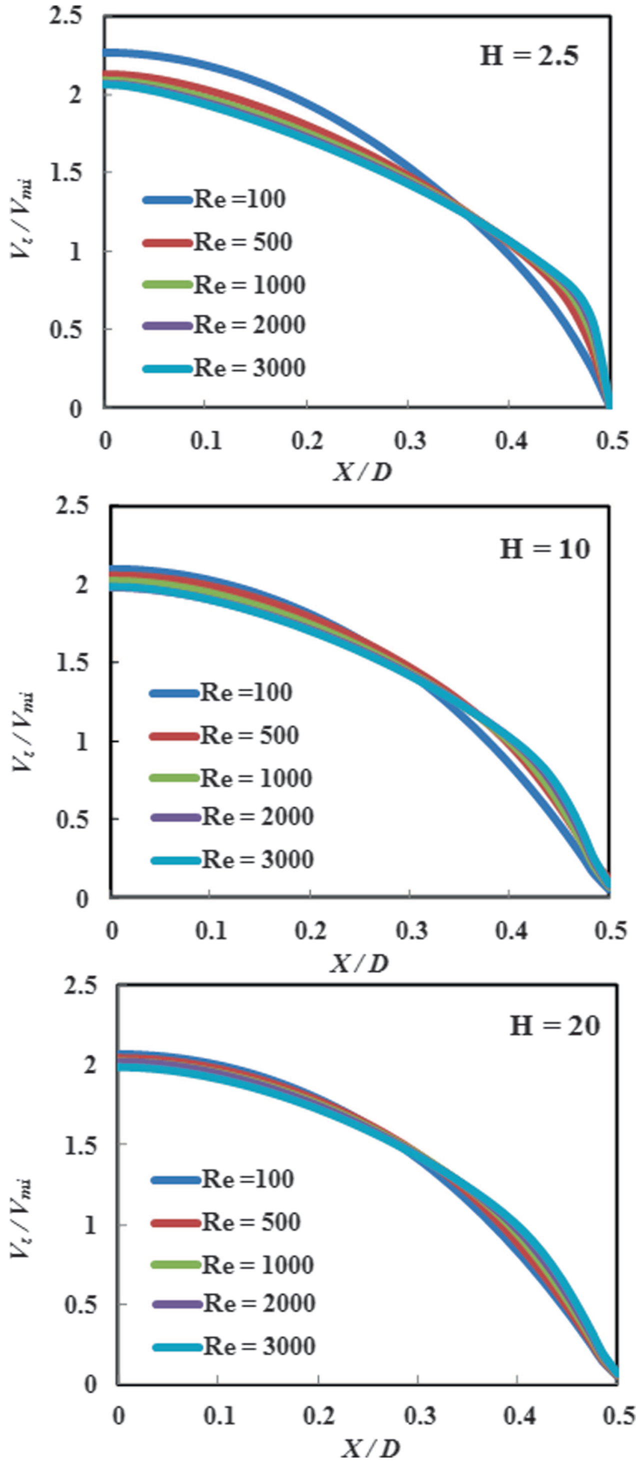

Figure 10. Effect of twist ratio on velocity in the direction of flow.

ratios. Contrary to straight square duct, where V_x and V_y components of velocity are nearly zero as compared to the V_z component, twisted duct shows comparable values for all three velocity components. V_x and V_y components of velocities observed are maximum for $H = 2.5$ and is about 2.56% of the inlet mean velocity. It is also seen that location of maximum value of V_x and V_y velocity components is in the region of $X/D = 0.3 - 0.5$, which is rather close to the wall. For a given twist ratio, as *Re* is increased, the location of maximum value of *x* and *y* components shifts towards the wall. For a given Reynolds number, as twist ratio is decreased, the location of maximum of *x* and *y* components shifts towards the wall. *X* and *y* components of velocity generated (also referred to as secondary flow) are the result of swirling motion occurring inside

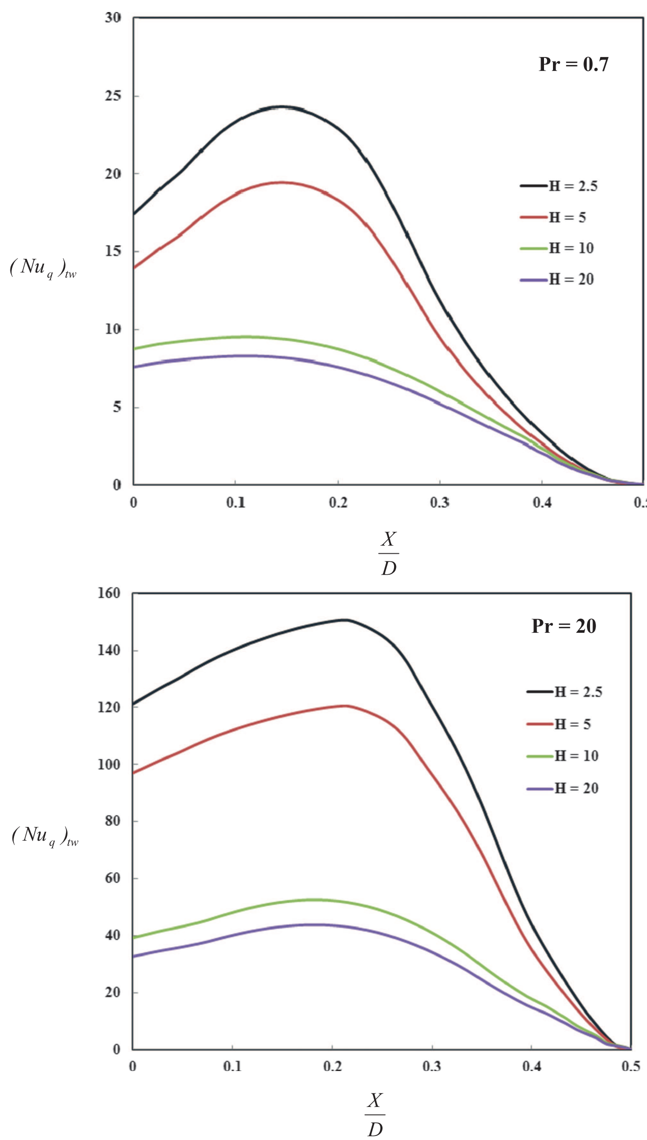

Figure 11. Effect of twist ratio on heat transfer along wall *(cb)* for $Re = 3000$.

the twisted tube. As magnitude and location of secondary flow are function of *Re* and twist ratio, shear stress at the wall (and hence *f.Re* value) will also be a function of the same. Observation leads to the conclusion that swirling motion (secondary flow) is responsible for higher *f.Re* values and its distribution at a given cross section in the case of twisted duct.

6.2 *Local heat transfer variation*

In the earlier section, it was found that $\overline{(Nu_q)}_{tw}$ values for twisted square ducts were dependent on *Re* and *Pr* values. In this section, local Nusselt number variation along the wall has been analysed. Figure 11 shows the effect of twist ratio on local Nusselt number for Re of 3000. It is observed that at given *Pr*, decreasing the *H* increases the heat transfer. Figures 12 and 13 show

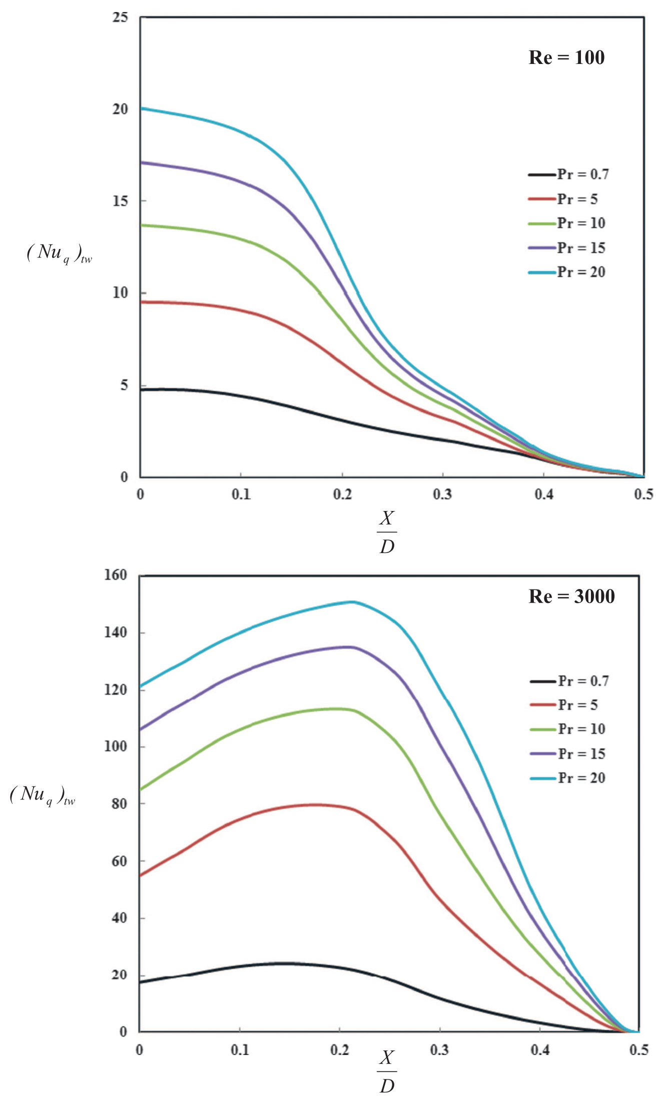

Figure 12. Local heat transfer solution at wall (cb) for $H = 2.5$.

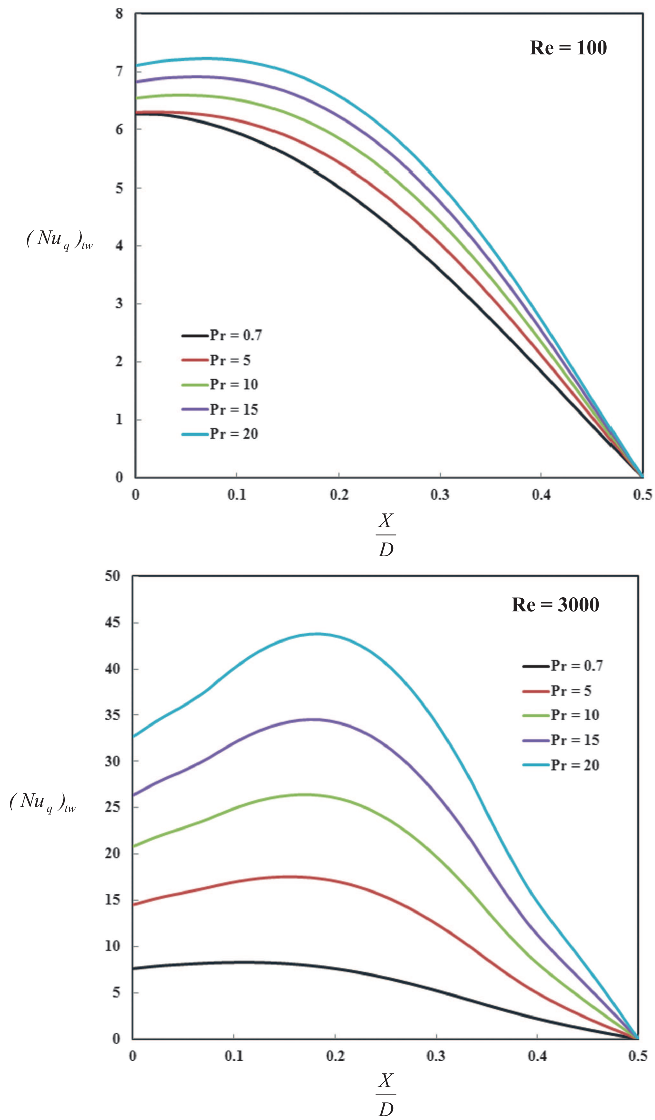

Figure 13. Local heat transfer solution at wall (cb) for $H = 20$.

$(Nu_q)_{tw}$ solutions for twist ratio 2.5 and 20, respectively. It is seen that location of maximum $(Nu_q)_{tw}$ is not at the center of edge (point *c*) as expected for straight duct. Location of maximum $(Nu_q)_{tw}$ point depends upon H and Re. Location of maximum $(Nu_q)_{tw}$ point shifts away from point *c* with an increase in the magnitude of secondary flow. This is an important observation as it will determine the location of maximum heat flux point on duct wall.

6.3 *Comparison of numerical results with straight square duct*

The suitability of a square twisted duct can be judged by comparing increase in heat transfer to increase in pressure drop, with respect to straight square duct. The friction factor and Nusselt number for twisted square duct are normalised with the friction factor and Nusselt number of the straight square duct for identical pumping power criteria. Eq. (10) gives the basis for comparison. Eq. (11) gives *Re* of straight duct corresponding to *Re* of twisted square duct. Average friction factor and Nusselt number values for straight square duct are computed by using Eqs. (12) and (13), respectively, from Incropera & Dewitt (1996).

$$\left(\frac{\mathrm{m}}{\rho}\Delta\mathrm{P}\right)_{\mathrm{tw}} = \left(\frac{\mathrm{m}}{\rho}\Delta\mathrm{P}\right)_{\mathrm{st}}. \tag{10}$$

This leads to

$$Re_{st} = \left(A_r \frac{\overline{\mathrm{f_{tw}}}}{\overline{\mathrm{f_{st}}}} Re_{tw}^3\right)^{\frac{1}{3}} \tag{11}$$

$$\overline{\mathrm{f_{st}}} = \frac{14.2}{\mathrm{Re}} \quad \text{for Re} \leq 3000 \tag{12}$$

$$\overline{\mathrm{Nu_{q_{st}}}} = 3.6 \quad \text{for Re} \leq 3000. \tag{13}$$

6.4 *Heat transfer enhancement*

In the earlier sections, it is realised that average $\overline{(f\,\mathrm{Re})}_{tw}$ and $\overline{(Nu_q)}_{tw}$ values in twisted duct are found to be higher than straight duct. Hence suitability twisted square duct can be better judged by comparing heat transfer enhancement with respect to rise in friction factor values compared

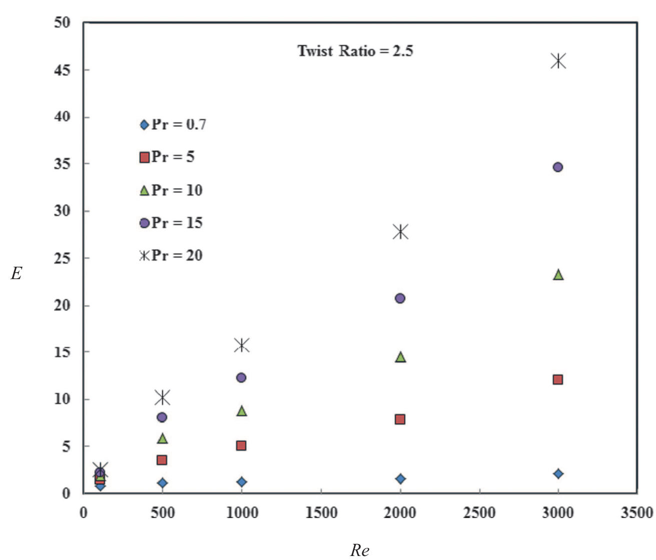

Figure 14. Suitability of twisted square duct for different fluids ($H = 2.5$).

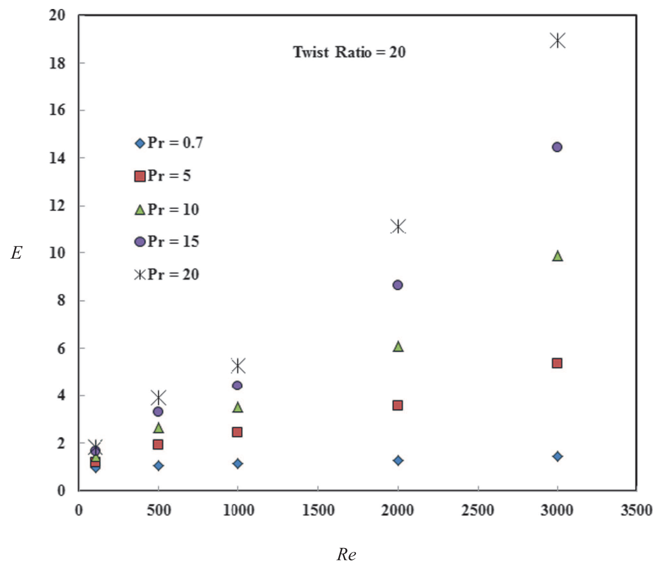

Figure 15. Suitability of twisted square duct for different fluids ($H = 20$).

to straight duct at constant pumping criteria. An Enhancement factor E can be defined, as shown by Eq. (14).

$$E = \frac{\dfrac{(\overline{\mathrm{Nu_q}})\mathrm{tw}}{(\overline{\mathrm{Nu_q}})\mathrm{st}}}{\dfrac{(\bar{\mathrm{f}}.\mathrm{Re})\mathrm{tw}}{(\bar{\mathrm{f}}.\mathrm{Re})\mathrm{st}}}. \tag{14}$$

Figures 14 and 15 show the suitability of twisted square duct for a wide range of fluids in the laminar flow regime. It is observed that in laminar flow, twisted square duct is a good choice for heat transfer enhancement for Prandtl number ranging from 0.7 to 20. Higher Pr fluids are more viscous fluids having larger momentum boundary layer thickness which obstruct flow of heat through convections. Swirl motion or secondary flow generated in twisted square duct decreases the resistance of momentum boundary layer for heat transfer. Therefore, large Prandtl number fluid shows more enhancements compared to lower Prandtl number fluids. It is observed that even H of 2.5 is not suitable for fluid with Pr of 0.7. However, a square twisted duct with a twist ratio of 20 can be used for higher Pr fluids. Hence selection of twisted duct for particular application will depend upon range of operating Re and Pr of fluid with design values of E to be kept in range of 1.5–2.

7. Conclusion

In the present work, fluid flow and heat transfer solution have been obtained for fully developed laminar flow with uniform wall heat flux boundary condition. Twist ratio used was 2.5, 5, 10 and 20. The Reynolds number range considered was 100–3000 and Prandtl number range was

0.7–20. For the first time, swirl parameter is defined for such type of flow. Average friction factor and Nusselt number are correlated in terms of swirl parameter, which is introduced for the first time for such flow. Maximum average Nusselt number is obtained with $H = 2.5$ at $Re = 3000$. Nusselt number was found to be a direct function of Re and Pr and inverse function of H. Local distribution of friction factor and Nusselt number are provided and it is found that the location of maxima changes with Reynolds number, Prandtl number and twist ratio. Comparison of heat transfer enhancement with respect to friction factor had been provided in terms of enhancement factor at constant pumping power. The maximum value of enhancement factor for $Pr = 0.7$ is 2.1, for $H = 2.5$ and $Re = 3000$. It is found that for the studied range of parameters, twisted tube enhances heat transfer hence it is a good substitute for straight tube in heat exchange equipments for operating under similar process conditions. These results will contribute towards development of energy efficient and compact heat exchangers.

Nomenclature

A	Heat transfer area, m^2
C	Specific heat of fluid, J/kg-K
D	Side of square, m
d	Hydraulic diameter of duct, m
E	Enhancement factor for a twisted square duct , dimensionless
f	Local friction factor $= \frac{\tau}{\left(\frac{\rho V_m^2}{2}\right)}$
$\bar{f}$	Average friction factor for cross section $= \frac{\tau_m}{\left(\frac{\rho V_m^2}{2}\right)}$
H	Twist ratio, dimensionless $\left(\frac{S}{d}\right)$
h	Heat transfer coefficient, W/m^2- K
k	Thermal conductivity of fluid, W/m-K
L	Periodic length, m
Nu	Nusselt number, dimensionless $\left(\frac{q\,d}{(T_w - T_b)\,k}\right)$
$\overline{Nu}$	Average Nusselt number for cross section, dimensionless $\left(\frac{q_m\,d}{(T_w - T_b)\,k}\right)$
Pr	Prandtl number $\left(\frac{\mu C}{k}\right)$
q''	Wall heat flux , W/m^2
Re	Reynolds number $\left(\frac{\rho V_m d}{\mu}\right)$
S	Pitch of the twisted tube, m
Sw	Swirl parameter, dimensionless $\left(\frac{Re}{\sqrt{H}} A_r\right)$
T	Temperature, K
V	Flow velocity (Twisted tube), m/s

Greek letters

μ	Dynamic viscosity , N-s / m^2
ρ	Density of fluid , kg/m^3
τ	Local wall shear stress, N/m^2

Subscript

a	Area averaged
b	Bulk temperature, fluid
i	Inlet
m	Mean
q	Constant wall heat flux boundary condition
r	Ratio
st	Straight duct
t	Thermal
tw	Twisted tube
w	Wall

Abbreviations

CFD	Computational fluid dynamics

References

Bishara F 2010 *Numerical simulation of fully developed Laminar flow and Heat transfer in Isothermal Helically Twisted tubes with Elliptical cross-section,* M.S. Thesis, University of Cincinnati, Cleveland state, USA

Chang K S, Choi J S and Kim J S 1988 Laminar fluid flow in a Twisted Elliptic tube. *KSME J.* 2(1): 44–51

Incropera F P and Dewitt D P 1996 *Fundamentals of heat and mass transfer*, fourth edition, John Wiley and Sons, pp. 419–481

Manglik R M and Bergles A E 1993 Heat transfer and pressure drop correlations for twisted - tape inserts in isothermal flows. *J. Heat Transfer* 115: 881–889

Masliyah J H and Nandakumar K 1981a Steady laminar flow through twisted pipes – fluid flow in square tubes. *ASME J. Heat Transfer* 103(4): 785–790

Masliyah J H and Nandakumar K 1981b Steady laminar flow through twisted pipes – heat transfer in square tubes. *ASME J. Heat Transfer* 103(4): 791–795

Todd L 1977 Some comments on steady laminar flow through twisted pipes. *J. Eng. Mathematics* 11: 29–48

Xu C G and Fan D N 1986 Some remarks on the helical Cartesian coordinates system and its application. *ASME J. Heat Transfer* 108: 483–486

Yang S, Zhang L and Xu H 2011 Experimental study on convective heat transfer and flow resistance characteristics of water flow in Twisted Elliptical tubes. *Appl. Thermal Eng.* 31(14–15): 2981–2991